chemengineering

MDPI

Article

Swift Removal of the Heavy Metals Cadmium and Lead from an Aqueous Solution by a CAN-Zeolite Synthesized from Natural Clay

Lobna Aloui [1], Soumaya Mezghich [2], Lamjed Mansour [3], Sana Hraiech [4] and Fadhila Ayari [1,*]

[1] Faculty of Sciences of Bizerte, LR 05/ES09 Laboratory of Applications of Chemistry to Resources and Natural Substances and to the Environment (LACReSNE), Carthage University, Zarzouna 7021, Tunisia
[2] Institute of Chemistry of Clermont-Ferrand (ICCF), Clermont Auvergne University, CNRS, BP 10448, F-63000 Clermont-Ferrand, France
[3] Department of Zoology, College of Science, King Saud University, Riyadh 11451, Saudi Arabia; lmansour@ksu.edu.sa
[4] Physical Chemistry Laboratory of Mineral Materials and Their Applications, National Center of Research in Materials Sciences, B.P. 73, Soliman 8027, Tunisia
* Correspondence: fadhila.ayari@ipeib.ucar.tn

Abstract: CAN-zeolite was synthesized with a high purity from natural kaolinite via alkali fusion by hydrothermal treatment at a pressure of 1 kbar H_2O. It was characterized by X-ray diffraction (XRD), scanning electron microscopy (SEM), infrared spectroscopy and nitrogen adsorption at 77 K. The results show that after AK hydrothermal treatment (under specific conditions), the SBET increases from 5.8 m^2g^{-1} to 30.07 m^2g^{-1} which is six times greater. The AK which was a non-porous or macroporous solid (the nitrogen adsorption/desorption of AK is of type II) became mesoporous (N_2 adsorption–desorption isotherms exhibit typical hysteresis of type IV) with a pore size of 5.9 Å. XRD of AK shows the presence of quartz (Q) as impurities, and illite and kaolinite as major fractions; after hydrothermal treatment, the XRD diffractogram shows only fine pics related to CAN-zeolite (with a good crystallinity), confirming the success of the synthesized process. These results suggest that the synthesized CAN-zeolite has the potential to be tested in the removal of heavy metals from waste water as part of a remediation process. Batch reactors were used to evaluate the adsorption isotherms and kinetic studies of heavy metals, cadmium, and lead, by natural kaolinite clay (AK) and synthesized cancrinite zeolite (CAN-zeolite). The results show that the adsorption kinetics of the bivalent heavy metals cadmium and lead are extremely fast with either AK or CAN-zeolite. Equilibrium was reached within 2 min. Adsorption isotherms show that the synthesized CAN-zeolite has a higher adsorption capacity; the retention capacity of lead and cadmium was three times greater than that presented by the natural clay mineral. According to the findings, CAN-zeolite has a higher affinity for PbII (192 mg/g) compared to CdII (68 mg/g). The negative reactive surface sites interacting with these cationic heavy metals resulted in a higher amount of heavy metals adsorption than the cation exchange capacity (CEC). The adsorption information was analyzed using the Langmuir and Freundlich equations. The Langmuir model provided a good fit to the equilibrium data, indicating a monolayer adsorption mechanism.

Keywords: heavy metals adsorption; zeolite; kaolinite; hydrothermal treatment

Citation: Aloui, L.; Mezghich, S.; Mansour, L.; Hraiech, S.; Ayari, F. Swift Removal of the Heavy Metals Cadmium and Lead from an Aqueous Solution by a CAN-Zeolite Synthesized from Natural Clay. *ChemEngineering* **2023**, *7*, 113. https://doi.org/10.3390/chemengineering7060113

Received: 7 September 2023
Revised: 11 November 2023
Accepted: 23 November 2023
Published: 30 November 2023

1. Introduction

The occurrence of heavy metals in industrial effluents, often in diverse and significant quantities, poses a substantial problem for human health and the environment. From a biological point of view, heavy metals can be divided into essential metals and toxic metals according to their physiological and toxic effects. Essential metals are essential trace elements for many cellular processes and are very low in biological tissues [1]. Some may

become toxic when the concentration exceeds a certain threshold such as molybdenum (Mo), selenium (Se), vanadium (V), titanium (Ti) and arsenic (As). Zinc, for example, is an oligo- (dehydrogenases, proteinase, peptidase) and has a significant role in the metabolic processes of proteins, carbohydrates and lipids, but it becomes toxic at a concentration of 1 molar [2]. Toxic metals are polluting with toxic effects on living organisms even at low concentrations. They have no known beneficial effects for the cell and include lead (Pb), mercury (Hg), cadmium (Cd) and antimony (Sb) [3]. The term "heavy metal" also implies a notion of toxicity. The term "trace metallic elements" is also used to describe these elements, as they are often found in very small quantities in the environment [4].

Cadmium is considered one of the most dangerous heavy metals and is frequently encountered in wastewater, particularly originating from metal plating, Cd–Ni batteries, phosphate fertilizers, mining, pigments, stabilizers and alloy production [5–7]. The World Health Organization has established a rigorous limit for cadmium in drinking water at 0.003 mg/L [8]. Since 1950, cadmium has been recognized as highly toxic in all its forms (metal, steam, salts and organic compounds). The presence of cadmium in water has been linked to kidney problems and heightened tension. Moreover, it is widely considered to be a teratogenic and carcinogenic agent (IARC) [9].

In the long-term lead contributes to a disease called "lead poisoning". It may have effects on the nervous, hematopoietic and cardiovascular systems [10]. High doses of lead in the body can lead to various neurological, renal and hematological disorders. In children, it can cause cerebral developmental disorders, with learning disabilities and psychological disruptions.

Lead can also disrupt different physiological processes at high doses and cause blood anemia and kidney effects (kidney failure). Lead has a range of negative impacts on the central nervous system such as developmental delay, irritability, sleep disorders and loss of memory. Additionally, it has long-term effects on the fertility of men. The effects of lead are generally amplified in the fetus and the child (congenital abnormalities, long-lasting neurobehavioral deficits).

On the other hand, the International Agency for Research on Cancer (IARC) has classified it with its inorganic derivatives in Category 2B (potentially carcinogenic to humans).

Various techniques have been devised for eliminating Cd, Pb and heavy metals from wastewater, including chemical precipitation, ion exchange, solvent extraction, reverse osmosis and membrane filtration [11]. Nevertheless, these approaches exhibit certain disadvantages, including incomplete removal of metal ions, elevated reagent and energy demands, the production of hazardous sludge and protracted desorption periods. Adsorption is widely recognized as a cost-effective and efficient approach to metal ion removal. Presently, numerous research endeavors are directed toward the development of natural, renewable and budget-friendly adsorbents, such as clays [12] and zeolites [13–18].

Within this array of materials, clays and zeolites stand out as cost-effective options with significant potential as adsorbents. Zeolites, in particular, hold a prominent position due to their porous three-dimensional structure, enhanced cation exchange capacity (CEC), outsize surface area and distinguished structural attributes, making them crucial materials in the realm of wastewater treatment.

Zeolites have a wide range of applications, in environmental cleanup, catalysis, biotechnology, gas sensing and medical purposes. Despite the abundance of naturally occurring zeolites, there is a growing focus on synthesizing zeolites due to their ease of production in a pure form, enhanced ion exchange ability and consistent size maintenance. Furthermore, producing zeolites from cost-effective sources, like rice husk, and clay has gained significant attention [19–21].

Zeolites are renowned for their excellent adsorption properties, enabling them to efficiently adsorb and exchange metal cations with positive charges within their structure. Several studies have investigated the use of both natural and synthetic zeolites as ion exchangers for the removal of heavy metals [22–25]. In comparison to their natural counterparts, synthetic zeolites exhibit high levels of purity, a uniform crystal size and are

well-suited for specific industrial applications. On the other hand, natural zeolites typically contain various impurities and lack a consistent crystal size [21].

Cancrinite (CAN), which is a low-silica zeolite (Si/Al = 1.5), can be hydrothermally synthesized from gels containing cations such as Na^+ and anions such as CO_3^{2-} and OH^-. Cancrinite accommodates a wide range of both anions and exchangeable cations in the micropore [26]. The merit of the cancrinite structure can therefore be utilized for adsorption of heavy metals.

Within the scope of this investigation, CAN-zeolite was prepared by hydrothermal alkali-activation of aluminosilicate materials at appropriate temperatures and pressures in high-pressure autoclaves.

The chemical and morphological composition of the produced adsorbent underwent examination through techniques such as X-ray diffraction (XRD), scanning electron microscopy (SEM) and N_2 adsorption/desorption isotherms. Subsequently, the zeolite composite created in this manner was assessed for its effectiveness as an adsorbent in removing cadmium and lead heavy metal from aqueous solution. According to the World Health Organization, the acceptable limits of some heavy metal ions in drinking water are as follows: Pb (50 μg L^{-1}), Cd (5 μg L^{-1}) [27].

Kinetic and adsorption isotherms were determined. The Langmuir isotherm was employed to ascertain the anticipated greatest adsorption capacity, and ΔG thermodynamic parameters was assessed.

These findings underscore the value of creating cost-effective water purification composite adsorbents derived from locally sourced materials.

2. Experimental

2.1. Materials

The $CdCl_2$ $2.5H_2O$ and $Pb(NO_3)_2$ used in these study were obtained from the Aldrich-Sigma chemical company.

Clay mineral was used in this investigation, kaolinite, provided from Ghardimaou (North West of Tunisia) and denoted AK. The sample taken underwent the following unit operations:

- Crushing of the sample rocks into pieces using a mortar;
- Drying in the oven for 24 h (T = 308 K);
- Grinding pieces of the clay sample in a grinder;
- Sieving the sample powder (50 μm sieve).

Prior to utilization, the clay underwent a purification process to eliminate organic matter and impurities. This involved adding 0.1 M of HCl to the clay suspension (20 g of raw AK mixed with distilled water). The mixture was agitated for 12 h until it reached complete homogenization. The fine fraction, characterized by particle sizes less than 2 μm, was isolated by centrifugation at 4000 tr.min^{-1}, a process repeated five times. The clay was subsequently rinsed with distilled water until the supernatant was free of chloride ions, as confirmed by the $AgNO_3$ test. The resulting sample was then dried at 353 K, crushed and passed through a 63 μm mesh sieve. The AK obtained through this process was used in the synthesis of CAN-zeolite.

2.2. Preparation of Cancrinite Zeolite

CAN-zeolite was synthesized by the conventional alkaline fusion method prior to hydrothermal treatment using kaolinite clay (AK) (Figure 1). For that, 10 g of AK was subjected to heating at 923 K for a duration of 2 h within an air-filled furnace. The resulting amorphous solid (referred to as AKC) was subsequently blended with 250 mL of NaOH solution (4 M) and subjected to another 2 h heating period at 923 K in the furnace.

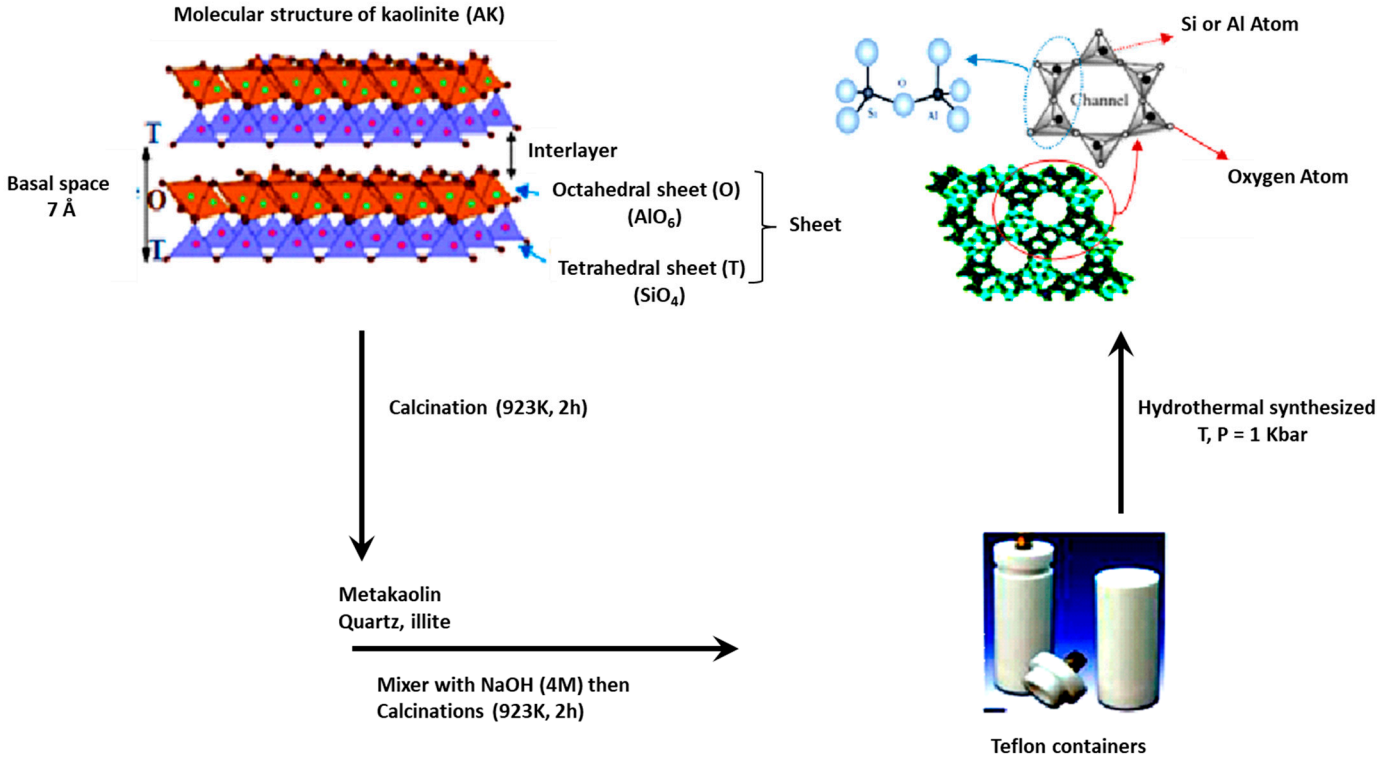

Figure 1. Protocol of CAN-Zeolite synthesis [28,29].

The AKC powder was allowed to cool and then underwent a grinding process. Subsequently, this powder was introduced into Teflon containers, which were filled with distilled water. These Teflon containers were then sealed and positioned inside a high-pressure autoclave (Autoclave Engineers unit from the USA, measuring 6 cm in length and 3 cm in width). They were securely closed and positioned vertically within a furnace, where they remained for a period of 21 days within the temperature range of 403 K to 433 K.

Upon reaching the desired furnace temperature, an external water pressure was applied by means of a Sitec manual hydraulic piston pump (Switzerland). This pump was utilized to introduce distilled water into the autoclave at a water pressure of 1 kbar.

2.3. Characterization of Clay and Zeolite

Conventional methods were employed to characterize the samples (AK and CAN-zeolite). This included mineralogical analysis using X-ray diffraction (Leipzig, Germany, Bruker D-8 FOCUS diffractometer). Data collection was carried out in the 2θ range of 0–60°. Additionally, the chemical composition of the samples was determined through energy dispersive X-ray analysis (EDAX), enabling a semi-quantitative assessment of their chemical composition under specific conditions. To examine their morphology, a scanning electron microscope (SEM) was employed (SEM) (FEI Quanta 200, Hillsboro, OR, USA). Specific surface areas were calculated using the BET equation, employing nitrogen adsorption data obtained with a Micrometrics ASAP 2010 surface area analyzer.

For thermogravimetric analysis, we used a TA Instruments TGA Q500 instrument (New Castle, DE, USA) equipped with a furnace capable of reaching temperatures up to 1000 °C and various carrier gas options (Ar, He, N_2, Air…). The experiments were conducted under a dry air flow (100 mL/min) in a temperature range from 25 to 900 °C with a ramp rate of 5 °C/min. The mass of the adsorbent used was approximately 30 mg.

2.4. Kinetics Study

The adequate adsorption time is an important parameter to be determined in our work. Thus, to determine the equilibrium time of maximum adsorption, a series of adsorption experiments were carried out at different durations via a batch process.

In fact, the adsorption kinetics of Pb^{2+} and Cd^{2+} were carried out by adding 50 mg of adsorbent to 20 mL of a known-concentration solution of each adsorbate ($[Cd^{2+}] = 10^{-3}$ M) and ($[Pb^{2+}] = 0.510^{-3}$ M) respecting the maximum quantities that can be present in the discharge water. These solution were prepared by utilizing a stock solution of $CdCl_2.2.5H_2O$ and $Pb(NO_3)_2$ at 0.1 mol L^{-1}. The agitation time ranged from 1 min to 2 h; after agitation in a thermostatic orbital shaker at room temperature, the solutions were filtered and the resulting filtrates were analyzed using appropriate wavelengths in atomic absorption spectroscopy. Blank samples (without solids) were prepared to confirm that there was no adsorption onto the used filters. Filtration allowed quick analyses compared to centrifugation.

The amounts of each adsorbed heavy metal (Q_{ads}) were calculated by the following relations (Equation (1)):

$$Q_{ads} = \frac{(C_0 - C_e)V}{m} \quad (1)$$

C_0 and C_e (or C_{eq}) are the initial and equilibrium concentrations of heavy metal (mg L^{-1}), respectively. V is the volume of the heavy metal solution (L) and m is the mass of the adsorbent (g).

2.5. Adsorption Isotherms of Cd and Pb by Clay and CAN-Zeolite

Batch experiments were conducted using bottles containing 10 mL of Cd(II) and Pb(II) solutions with varying initial concentrations (those solutions were prepared by diluting a concentrated stock solution) along with 0.025 g of adsorbent (either clay AK or CAN-zeolite), then the samples were agitated in a thermostatic orbital shaker at room temperature (298 K). Upon reaching equilibrium, the adsorbent was separated by centrifugation at 7000 rpm.min^{-1}. The initial and final concentrations of heavy metals within the solutions were determined through atomic absorption spectroscopy. The quantity of heavy metal adsorbed when the system reached equilibrium, $Q_e = Q_{ads}$ (mg/g), was determined (Equation (1)).

The pH levels before and after adsorption were measured fell within the range of 6 to 6.7; no significant variation was noted.

3. Results and discussion

3.1. Characterization of Purified Kaolinite Clay before and after Heating and NaOH Treatment

Elemental chemical analysis of the clay sample was carried out using a Fluorescence Spectrometer X of the "Axion" type, with 1 kW wavelength dispersion.

The chemical compositions of AK are detailed in Table 1. Based on the aforementioned result and referring to some reviews [17,30,31], it is evident that this sample is an aluminosilicate source with a Si/Al molar ratio 1.24 (Table 1) since the results indicate that the predominant constituents are Silica and Alumine.

Table 1. Purified kaolinite composition.

Element	O	Na	Mg	Al	Si	K	Ti	Fe	Si/Al
% atomic	45.74	21.54	0.57	13.70	16.99	0.70	0.16	0.60	1.24

The percentage of silica and alumina is very significant, indicating the presence of kaolinite ($Al_2Si_2O_5$ $(OH)_4$) [22,32].

X-ray diffraction analysis was employed to examine the structural characteristics of the used clay mineral before and after treatment.

The results show the presence of quartz (Q) as an impurity (peaks at 3.34 Å and 4.25 Å (Figure 2a)) which disappears after heating the sample at 923 K (Figure 2b). Furthermore,

the XRD data (Figure 2a) indicate that the clay mineral is predominantly composed of illite (Il), as evidenced by the peaks at 10 Å, 4.97 Å and 2.57 Å, associated to the kaolinite (K) fraction [22,24,32], identified by the appearance of peaks at 7.15 Å and 3.57 Å in the diffractograms, but these last peaks disappear after heating AK at 923 K (AK heated at 923 K was labeled AKC, Figure 2b).

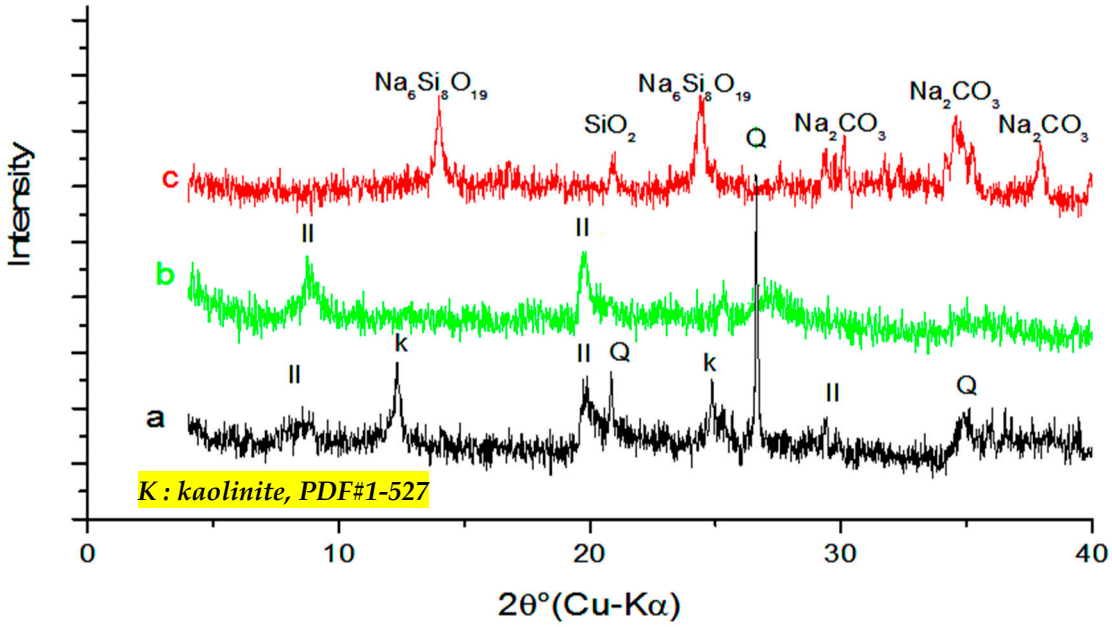

Figure 2. X-ray diffractograms of (**a**): the AK sample; (**b**): AK heated at 650 °C (AKC); (**c**): AKC heated at 650 °C treated with NaOH/AKC = 4.

Upon the addition of NaOH to AKC and calcination at 923 K (Figure 2c), we observe the complete dissolution of all clay mineral fractions and the formation of other phases, such as Na_2CO_3, SiO_2 and $Na_6Si_8O_{19}$. These formed phases could serve as promising materials for the synthesis of CAN-zeolite.

IR spectroscopy characterization of AK (Figure 3) reveals broad bands at around 3639 and 3713 cm^{-1} which are characteristic of the OH-stretching vibrations of the illite and kaolinite phases [33], they correspond to the vibration in the plane of Al-Si-O and the mode of deformation of Mg-Al-OH in illite. The absorption band around 3450 cm^{-1} has been attributed to the OH frequencies of the water molecule adsorbed in the clay surface. The band at 1650 cm^{-1} corresponds to the bending mode of the water molecule [34]. After calcination (AKC), these different bands disappeared, confirming its amorphization. On the other hand, after calcination, the characteristic bands of Quartz, Si–O–Si vibrations which are located at around 800 and 1080 cm^{-1}, disappeared, supporting the X-ray analysis.

To examine AK morphology, a scanning electron microscope was employed (SEM). SEM imagery is essential to show the transformation of the morphological surface of AK after zeolite synthesis. The result displayed by Figure 4a shows small and large agglomerates of sizable particles. seemingly created through the aggregation of multiple flaky particles stacked together.

The specific area of clays is estimated by the **BET** method (**B**runauer, **E**mett and **T**eller) [34]. This technique consists of determining the adsorption isotherm of gaseous dinitrogen at a temperature close to its boiling point (77 K). To conduct these adsorption measurements, the sample surfaces must be well degassed and the adsorbed water must be removed to make the surfaces accessible to nitrogen molecules.

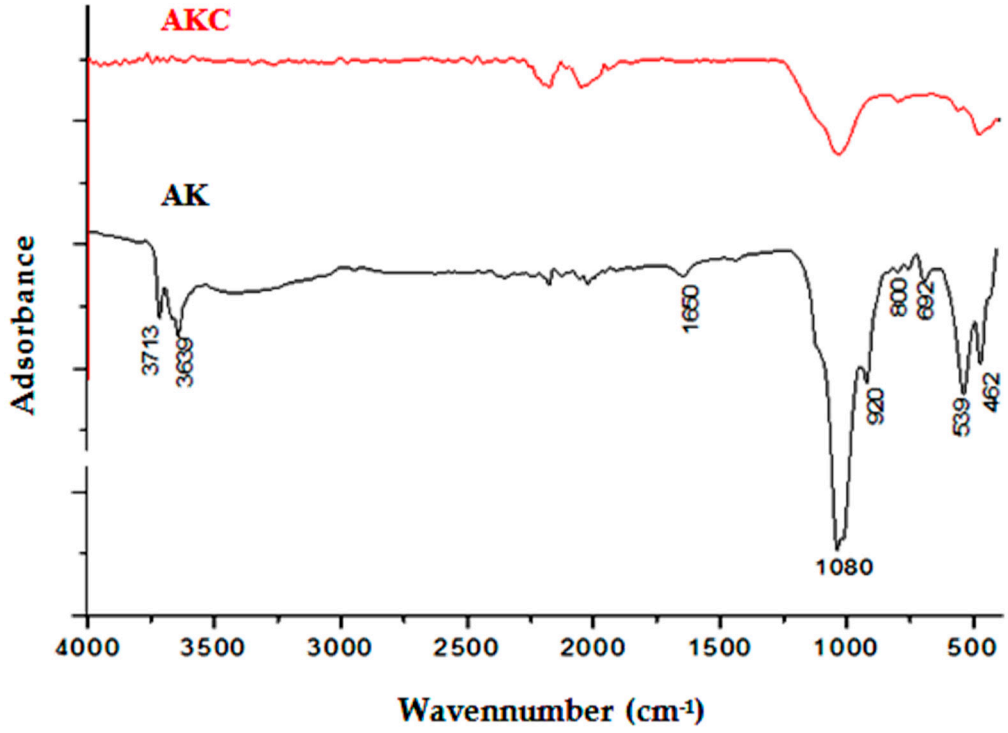

Figure 3. FTIR spectra of natural clay and heated clay after alkali fusion.

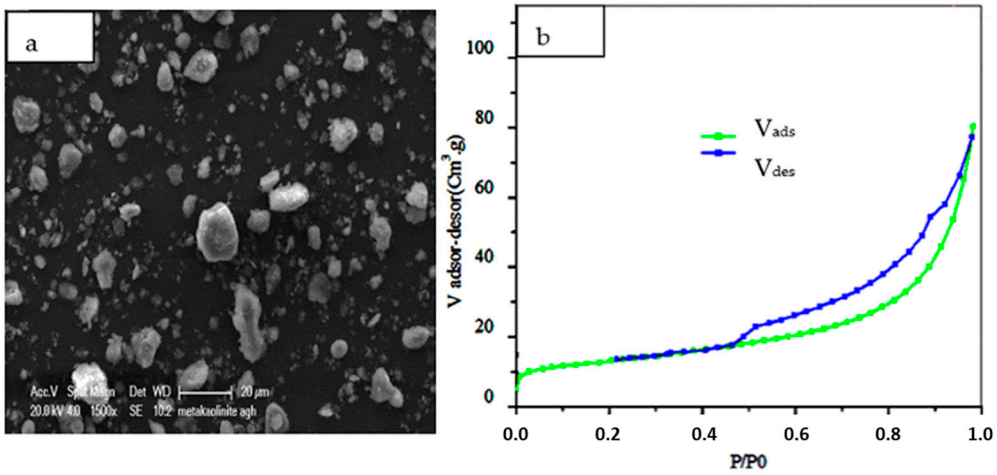

Figure 4. (**a**) SEM images of natural clay (AK); (**b**) N_2 adsorption–desorption isotherms of AK.

A total of 100 mg of AK clay sample is first subjected to pressure desorption reduction (<1 Pa), at a temperature between 160 and 250 °C overnight. The degassing temperature was chosen based on the TGA results.

In Figure 4b, we present the adsorption and desorption isotherms of dinitrogen on the AK clay sample studied.

The adsorption/desorption nitrogen isotherms for AK exhibit a type II behavior (Figure 4b). In accordance with the guidelines established by the IUPAC (International Union of Pure and Applied Chemistry), this isotherm is very widespread for non-porous or macroporous solids. The fact that there is no point clearly identifiable (corresponding to the filling of a monolayer) and a continuous increase in the adsorbed quantity is a sign of the energetic heterogeneity of the surface with respect to adsorbate/adsorbent interactions. In this case in AK, there is a superposition of monolayer and multilayer adsorption.

In addition, it is noted that the adsorption/desorption nitrogen isotherms for AK are characterized by a hysteresis loop but lacking a saturation plateau (Figure 4b), indicating a

non-rigid structure in this case [29,34]. This type of hysteresis (H3) is commonly observed in the case of platelet-shaped particles, which is the case for clays including slit-shaped pores. The specific surface area (S_{BET}) of AK clay is 5.85 cm^2 g^{-1}.

For thermogravimetric analysis (TGA), the study was conducted using a TGA Q500 instrument equipped with a furnace capable of reaching temperatures up to 900 °C. The temperature gradient was set at 5 °C/min.

The thermogram as shown in Figure 5 clearly demonstrates a high thermal stability of AK even at very high temperatures. Four mass losses are observed between 90 °C and 520 °C.

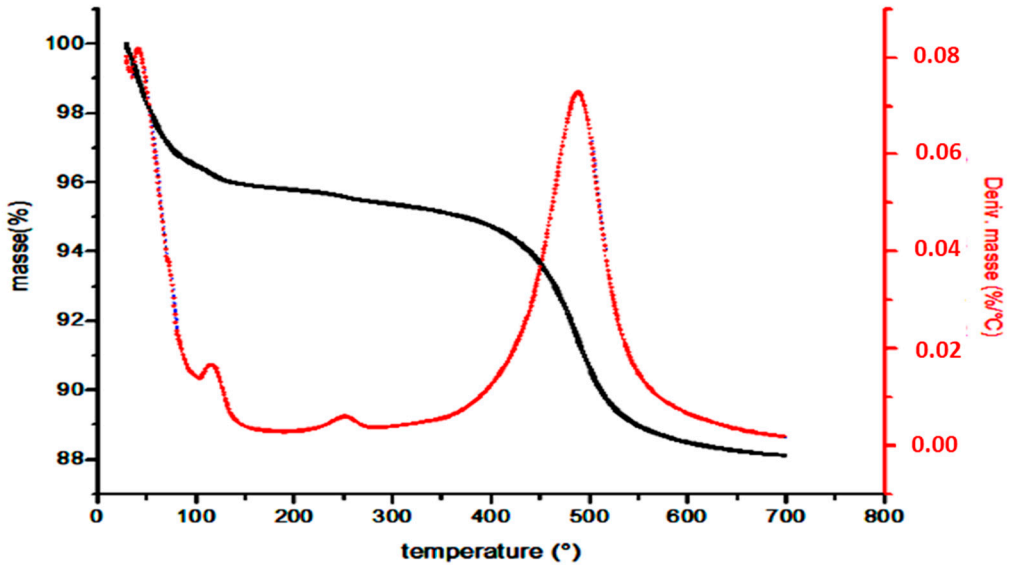

Figure 5. Thermogravimetric analysis of AK.

The first mass loss, occurring around 90 °C and more pronounced, indicates the loss of hydration water (dehydration).

A second mass loss at high intensity, typically extending from 400 °C to 700 °C, corresponds to the dehydroxylation of clay layers.

3.2. Characterization of Synthetic CAN-Zeolite

The X-ray diffraction pattern of the synthesized CAN-zeolite (Figure 6) shows a good crystallinity of the cancrinite sample suggested by the presence of reflections at 2θ angles of approximately 14°, 18°, 24°, 27°, and 33° [32,35,36]. These peaks point to the crystallization of the released aluminum and silicon components.

On the other hand, the FTIR spectrum of the synthesized zeolite (Figure 7) shows bands at 1445 and 1417 cm^{-1}, which suggests the presence of carbonates as anions occluded in the internal cavities of the cancrinite zeolite [12,35]. The bands observed at 1638 and 3450 cm^{-1} correspond to water molecules occluded inside the cancrinite structure [36]. The bands in the range of 1120–426 cm^{-1} correspond to the symmetric and asymmetric vibrations of atoms that form the structural units of the zeolite. Those bands are considered as the fingerprint of the zeolite, especially the asymmetric vibrations between 685 and 344 cm^{-1} [37].

The N_2 adsorption–desorption isotherms of the synthesized zeolites at high temperatures (Figure 8a) exhibit typical hysteresis of type IV, which suggests the presence of mesopores, though they may be predominantly intergranular.

However, the adsorbed quantities remain low for a mesoporous material. In fact, the pore size in cancrinite zeolite measures 5.9 Å (Figure 8c), which should be sufficiently large to accommodate N_2 molecules. Yet, the presence of intercalated carbonate in the cancrinite channels, as confirmed by FTIR (σ = 1445 cm^{-1}), obstructs them and restricts nitrogen adsorption to the external surfaces of the CAN zeolite. These results align with the literature [35,38].

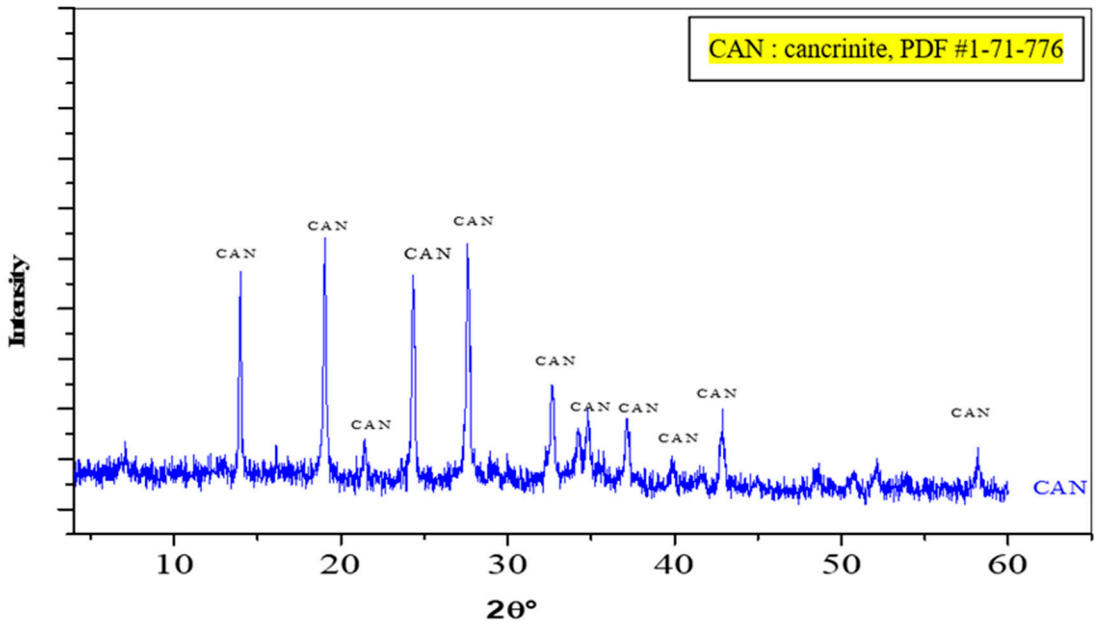

Figure 6. XRD pattern of synthesized CAN-zeolite.

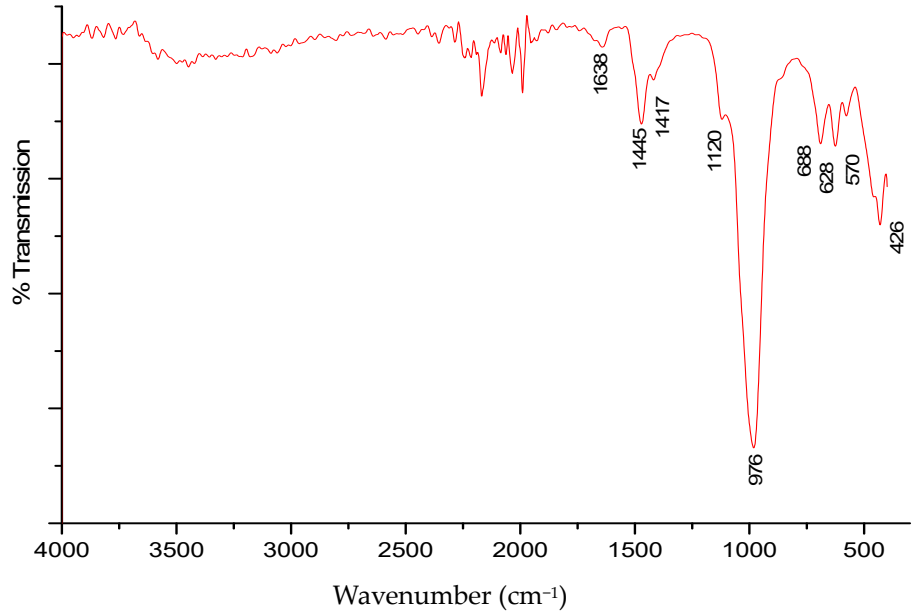

Figure 7. FTIR spectrum of synthesized CAN-zeolite.

The specific surface area (SBET) of CAN-zeolite is estimated (30.07 $m^2 \cdot g^{-1}$) using the **BET** (**B**runauer, **E**mmett, and **T**eller) method, and it was found to be higher than that of the used clay (5.85 $m^2 \cdot g^{-1}$): it was six times greater. This suggests that the synthesized CAN-zeolite holds potential for testing in the removal of heavy metals from wastewater as part of a remediation process.

The SEM imagery of CAN-zeolite is exhibited in Figure 8b. The results show the presence of crystals in the form of rods which correspond to the expected morphology of CAN-zeolite. The highly symmetric hexagonal needle or stick-like shapes observed are a suggestion of the cancrinite's hexagonal symmetry (P6), which is an indication of high crystallinity that aligns with some authors [35]. The syntheses are replicable and have been confirmed through three repetitions.

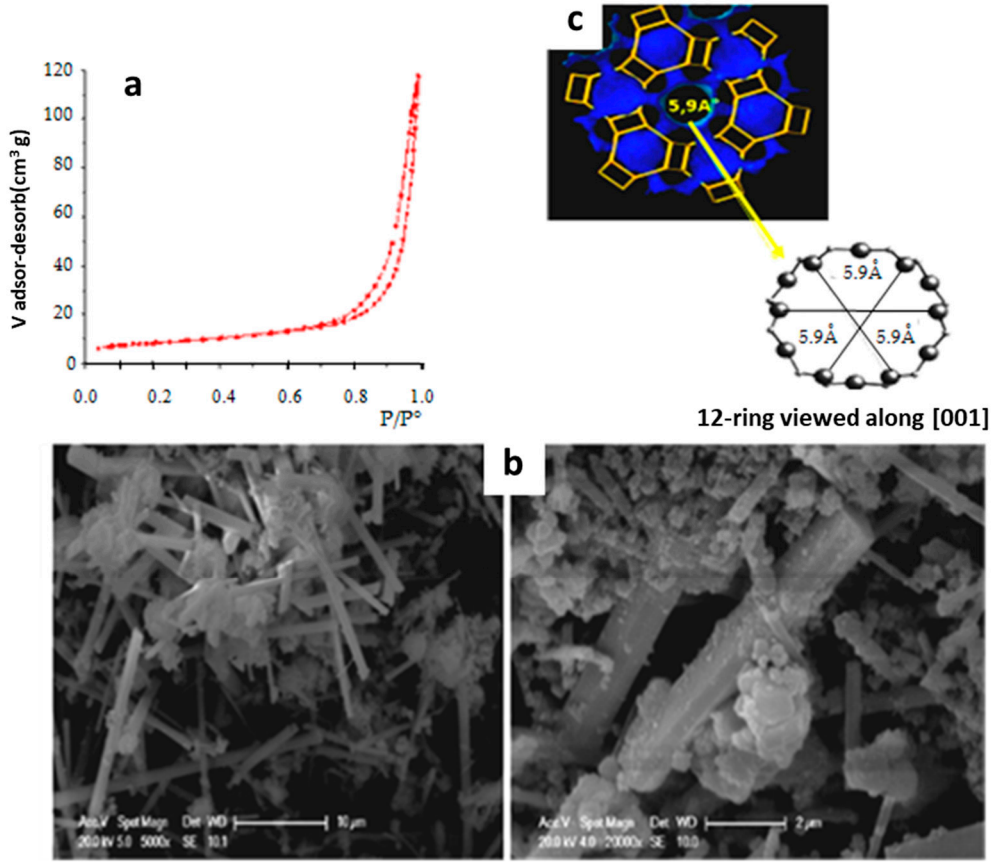

Figure 8. (**a**) N_2 adsorption–desorption isotherms, (**b**) SEM of CAN-zeolite, (**c**) CAN-zeolite structure (3D) [35,38].

The EDAX analysis (Figure 9) allowed us to determine the Si/Al ratio (Si/Al~1.5), a value that corroborates the findings from XRD and SEM. These results are in good agreement with those reported previously [35,38].

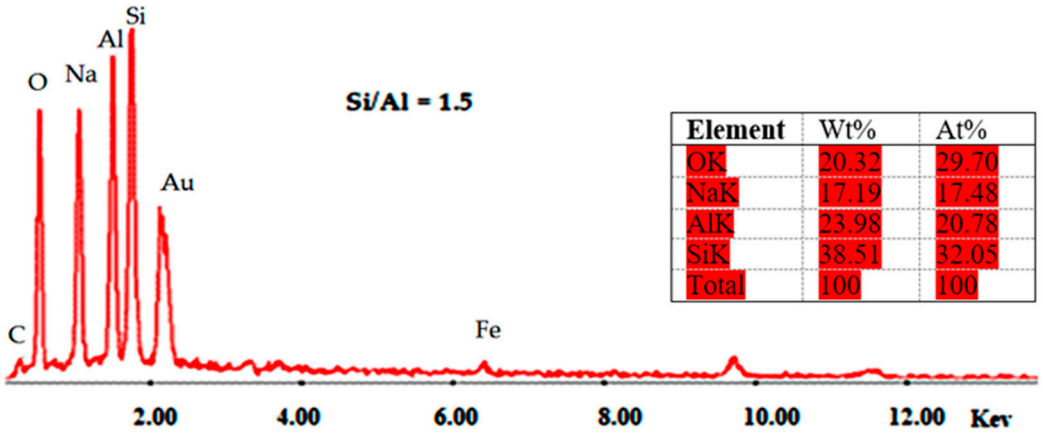

Figure 9. EDAX spectrum of the CAN-zeolite.

The thermogravimetric analysis of CAN-zeolite is illustrated (Figure 10), showing two regions: The first region between 40 °C and 400 °C is associated with water loss. The initial peak around 100 °C could be attributed to the dehydration of surface water on the CAN-zeolite. The peaks at approximately 180 °C and 230 °C are linked to the water loss from the cancrinite cages. The presence of two peaks could be explained by the heterogeneous nature of compensating cations in CAN, such as Mg^{2+}, K^+, Fe^{2+}, and Na^+.

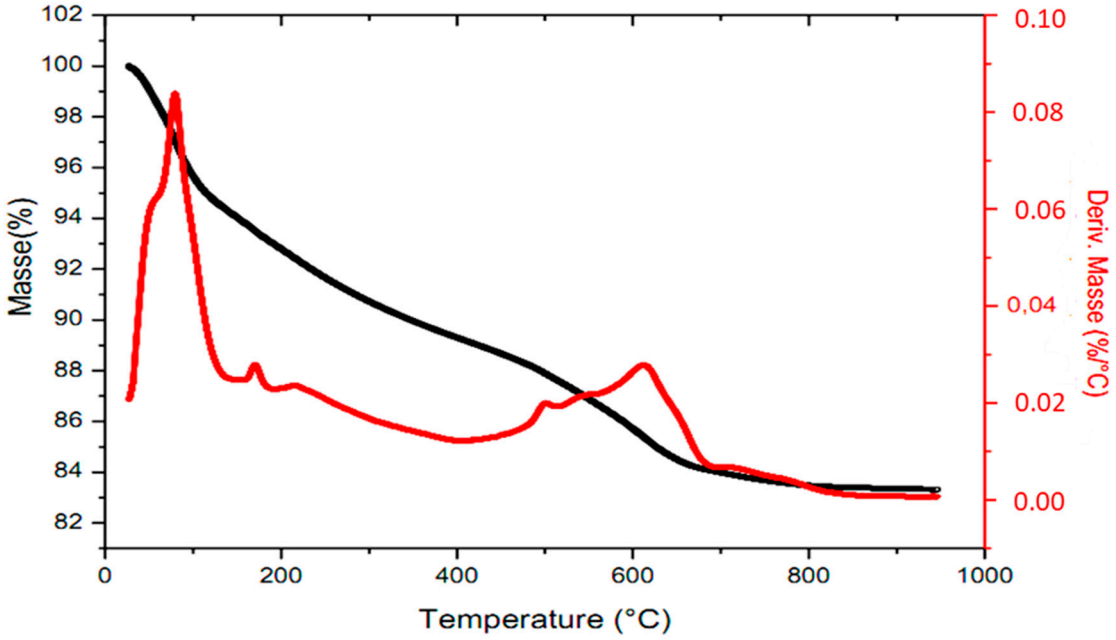

Figure 10. The thermogravimetric analysis of CAN-zeolite.

The second region at temperatures between 400 °C and 800 °C is associated with water loss from narrow pores and the decomposition of carbonates. The total weight loss is approximately 16% at 950 °C [34].

3.3. Cadmium and Lead Immobilization by AK and Synthesized CAN-Zeolite

3.3.1. Effect of Contact Time

The contact time for the adsorption capacity of cadmium and lead onto AK and CAN-zeolite has been studied (Equation (1), Figure 11a,b). The findings indicate a sharp initial increase in the adsorption quantity for both heavy metals, followed by a gradual rise until equilibrium was attained, which occurred around the 2 min mark. Several studies can be referenced in the same context [33,34,39,40]. Chen [40], Rybick [33], Gupta [34], and Kriaa [35] have shown in their previous work that the adsorption of cadmium and lead on various clay minerals and in different types of zeolites was achieved in over 20 min.

The phenomenon described above can be attributed to the abundance of empty surface sites available for adsorption during the initial phase. As time progresses, it becomes increasingly challenging for the remaining vacant surface sites to be occupied due to repulsive forces between the heavy metal ions in the aqueous solution and those present on the adsorbent surface [41]. According to the study of Muayad et al. [32], the existence of anionic components within the CAN-zeolite channel system significantly reduces the activation energy required for cation transport.

Several studies have shown that the required time to reach equilibrium, in the same experimental condition, is greater than that found in this investigation [19,32,42–45].

3.3.2. Cadmium and Lead Adsorption Isotherms

Adsorption isotherm experiments were conducted by introducing 0.025 g of adsorbants (AK and CAN-zeolite) into 10 mL of cadmium or lead solutions at desired concentrations. The mixture was agitated using a thermostatic shaking batch at 298 K for 60 min to reach saturation. The initial pH of the solution was approximately 6. To ensure there was no heavy metal precipitation, the pH after adsorption was controlled and it was found to be 7 in all cases. Based on the cation speciation diagram in the solution, the pH level at which precipitation occurs is 8 for Cd^{2+} and 7–8 for Pb^{2+}.

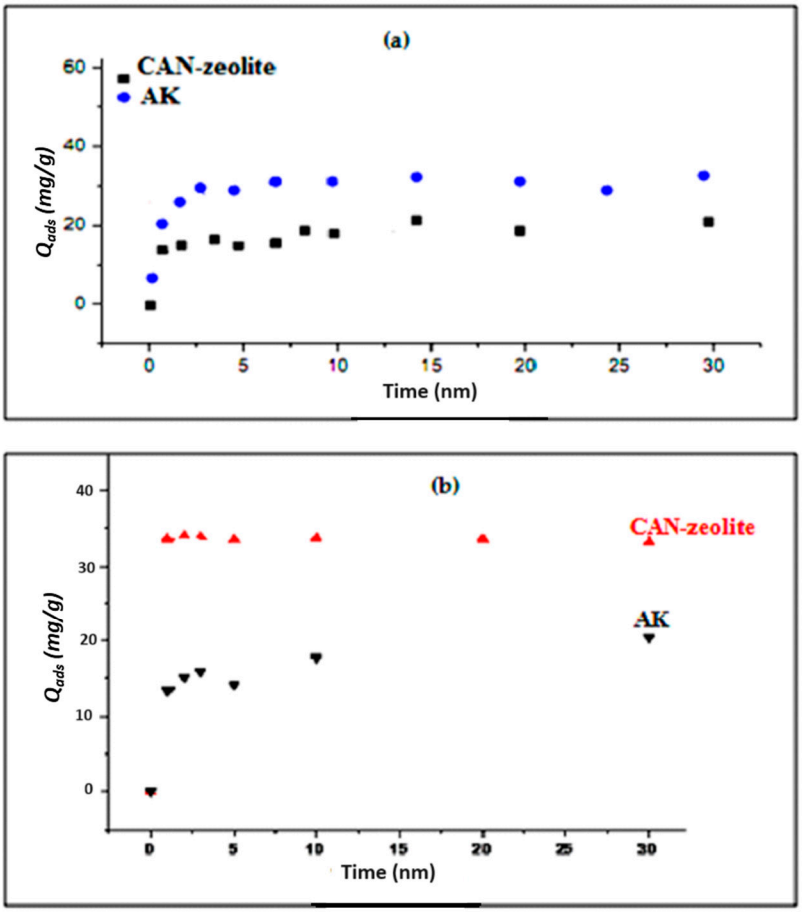

Figure 11. Effect of contact time for (**a**) cadmium adsorption and (**b**) lead adsorption on natural clay and synthesized CAN-zeolite, $[Pb]_I = 0.510^{-3}$ M, $[Cd]_I = 10^{-3}$ M, pH = 6.2, T = 25 °C.

The equilibrium adsorption of heavy metals (Q_e (mg g^{-1})) was performed using Equation (1).

The adsorption isotherms reveal differences in the adsorption capacities of cadmium and lead depending on the nature of the adsorbent matrix (Figure 12). The comparative study of these isotherms demonstrates the superiority of the CAN synthesized compared to the natural clay used.

For cadmium (Figure 12a), very high adsorbed quantities exceeding 60 mg·g^{-1} were obtained at low residual concentrations, indicating a strong affinity between Cd^{2+} and the synthesized CAN-zeolite. The amount of Cd^{2+} adsorbed by the synthesized CAN is threetimes higher than that adsorbed by AK used as a reagent for CAN-zeolite synthesis.

The lead adsorption isotherms exhibit the same characteristics as those of cadmium (Figure 12b). Specifically, we observe that the CAN-zeolite synthesized adsorbs four times more Pb^{2+} (192.7 mg/g) than AK. This type of zeolite demonstrates a Pb^{2+} adsorption capacity three times greater than the one (52.3 mg/g) reported by Borhade [41]. This difference is credited to variations in the structure and adsorption capacities of each adsorbent and to the good purity of our synthesized CAN-zeolite.

In this study, the adsorption capacity of CAN-zeolite for these heavy metals exceeds the value reported in the literature (Table 2). By analyzing the outcomes gathered from various experiments, we can infer that the CAN-zeolite synthesized from the AK reagent exhibits the highest affinity for these two heavy metals (Table 3).

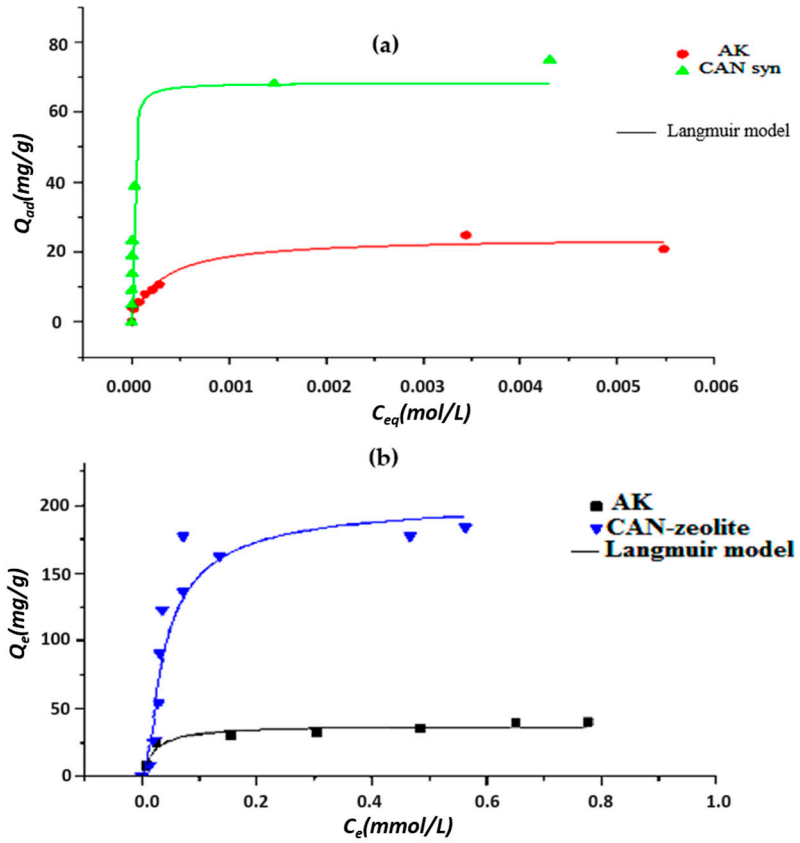

Figure 12. (**a**) Cadmium adsorptions isotherms; (**b**) Lead adsorptions isotherms on clays and CAN-zeolite, pH = 6.2, T = 25 °C.

It should be noted that the adsorption capacity and affinity of Pb^{2+} for these adsorbents are higher than those of Cd^{2+}. These findings align well with Coulomb's law; in this context, it is observed that the exchange affinity rises with the ion's valence. Additionally, when the charge is equal, the cation with a smaller hydrated radius is preferentially adsorbed: the hydrated radius of Pb^{2+} (0.401 nm) is smaller than that of Cd^{2+} (0.426 nm).

The experimental sorption data were correlated with the Langmuir model (Equation (2)):

$$Q_e = \frac{Q_m K_L C_e}{1 + K_L C_e} \tag{2}$$

Q_e (mgg^{-1}) is the amount of ions adsorbed per unit weight of adsorbents, C_e ($molL^{-1}$) is the equilibrium concentration, and Q_m and K_L are the Langmuir constants related to the capacity and energy of adsorption, respectively.

The Langmuir isotherm assumes (Figure 12) that the adsorption takes place at a homogeneous surface with all the adsorption sites having an identical adsorbate affinity. It was introduced to illustrate the monolayer sorption process. As can be seen from Figure 12a,b, the experimental adsorption data closely align with the Langmuir model, indicating a monolayer adsorption process for both heavy metals using either the AK or CAN adsorbents.

The free standard molar energy of adsorption $\Delta_{ads}G_m^0$ is performed using the following equation:

$$\Delta_{ads}G_m^0 = -RTLn(K_L) \tag{3}$$

R: universal gas constant = 8.314 $Jmol^{-1}$; T: temperature (K); K_L equilibrium constant of adsorption obtained from the Langmuir model.

The negative values of $\Delta_{ads}G_m^0$ (Table 3) indicate the spontaneity of the adsorption process of Pb^{2+} and Cd^{2+} by AK and CAN. This outcome aligns with prior research conducted by Sari [39], Kriaa [35], and Brodrade [41], which also observed the adsorption process to be spontaneous due to the negative value of the thermodynamic parameter: the Gibbs energy.

Table 2. Comparison study of CAN-zeolite adsorption capacity of cadmium and lead with different adsorbents.

Metal	Adsorbent	Q_{max} (mg g^{-1})	References
Cd(II)	Fe_2O_4-P(Cys/HEA) hydrogel	27.37	[13]
	Iron-modified zeolite	6.72	[13]
	Cancrinite	45.46	[33]
	Fly ash zéolithe X	97.78	[23]
	Kaolinite	9.9	[21]
	Nanocomposites	1.94	[46]
	Azide cancrinite	37	[41]
	Cancrinite	20.6	[41]
	Nanosillica	72.13	[47]
	Natural kaolin	24.17	This study
	Cancrinite zeolite	68.42	This study
Pb(II)	Cancrinite	52.3	[33]
	Cancrinite zeolite	90	[32]
	Fe_2O_4-P(Cys/HEA) hydrogel	39.06	[13]
	Fly ash zeolite	70.6	[48]
	Azid cancrinite	38.46	[41]
	Azide cancrinite	52.63	[33]
	Kaolinite	11.2	[22]
	Na-Bentonite	38	[48]
	Natural kaolin	37.97	This study
	Cancrinite zeolite	192.7	This study

Table 3. Estimated isotherms parameters for cadmium and lead adsorption.

Metal	Sample	Q_m (mg/g)	K_L	R^2	$\Delta_{ads}G_m^0$ (KJ·mol^{-1})
Cd(II)	AK	24.17	3357	0.952	−3.87
	Synthesized CAN	68.42	100,617.7	1	−28.53
Pb(II)	AK	37.973	47.633	0.884	−9.572
	Synthesized CAN	192.708	28.224	0.774	−8.275

3.4. Adsorption Mechanism

CAN has the formula Na_8 $(H_2O)_2CO_3$ $[Al_6Si_6O_{24}]$, whose channels contain anionic species such as CO^{3-}, OH^-, and sometimes $NO_3{}^{2-}$ [33,48]: these anionic species are not exchangeable with metal cations (Pb^{2+} and Cd^{2+}). The adsorption of heavy metals can be interpreted by the cation exchange phenomenon with sodium cations which play the role of compensating cations in the structure of the CAN-zeolite (Figure 13). By comparing the amounts of adsorbed lead and cadmium with respect to the amount of the CEC exchangeable sodium cations, we note that these adsorbed quantities are higher. This

difference can be explained by the adsorption on the surface of the CAN. The superior exchange which is accomplished with Pb^{2+} can be explained by the fact that lead has a smaller cation size in comparison to Cd^{2+} or by the formation of the lead clusters in the cages of the CAN-zeolite, since the lead is in the bivalent Pb^{2+} and monovalent Pb $(OH)^{+}$ forms in the studied pH.

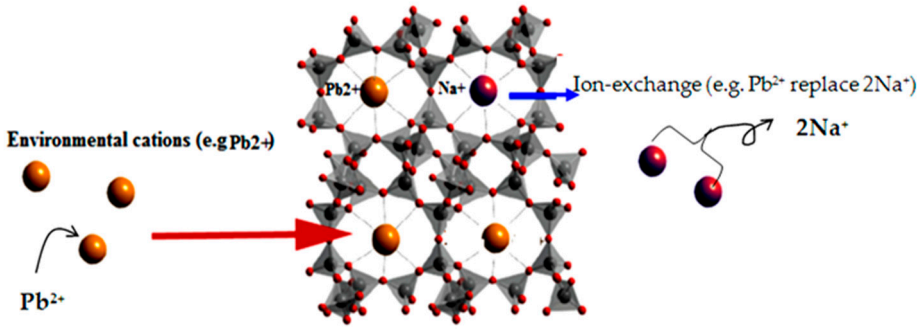

Figure 13. Structure of the CAN and mechanism of adsorption of heavy metals [26].

4. Conclusions

In this work, hexagonal cancrinite crystal was synthesized with a well-defined crystalline structure and a good purity, with Si/Al~1.5, from the natural kaolinite clay mineral.

Adsorption experiments revealed that cancrinite zeolites are considerably more effective than natural kaolinite at removing heavy metals such as lead and cadmium. According to the Langmuir isotherm model, the maximum adsorption capacity of Cd^{2+} and Pb^{2+} by cancrinite are three and four times higher than those noted for AK, respectively. Adsorption phenomena are governed by a monolayer mechanism. The kinetic adsorption is very fast (2 min) compared to the results presented in the literature. In conclusion, the nonporous material (CAN-zeolite) is an environmentally friendly and very low-cost material which will be a very promising candidate for heavy metal wastewater treatment for reuse.

Author Contributions: L.A.: Writing, review and editing; S.M. and S.H.: methodology, investigation, project administration; L.M.: participation in the characterization of initial materials; F.A., supervision, visualization, investigation, writing, review and editing. All authors have read and agreed to the published version of the manuscript.

Funding: This research received no external funding.

Data Availability Statement: The data presented in this study are available on request from the corresponding author.

Acknowledgments: The authors extend their appreciation to the Researchers Supporting Project number (RSP 2023R75), King Saudi University, Riyadh, Saudi Arabia.

Conflicts of Interest: The authors declare that they have no known competing financial interest or personal relationship that could have appeared to influence the work reported in this paper.

References

1. Loué, A. *Oligo-Eléments En Agriculture, 2nd ed*; SCPA (Société Commerciale des Potasses et de l'Azote): Nathan, Australia, 1993; pp. 45–177.
2. Kabata-Pendias, A.; Pendias, H. *Trace Elements in Soils and Plants*; CRC Press: London, UK, 2001.
3. Adriano, D.C. *Trace Elements in Terrestrial Environments: Biochemistry, Bioavailability and Risks of Metals*; Springer: Berlin/Heidelberg, Germany, 2001.
4. Baker, A.J.M.; Walker, P.L. Ecophysiology of metal uptake by tolerant plants. In *Heavy Metal Tolerance in Plants—Evolutionary Aspects*; Shaw, A.J., Ed.; CRC Press: Boca Raton, FL, USA, 1989; pp. 155–177.
5. Kannan, N.; Rengasamy, G. Comparison of cadmium ion adsorption on various activated carbons. *Water Air Soil Pollut.* **2005**, *163*, 185–201. [CrossRef]
6. Kumar, M.; Tripathi, B.P.; Shahi, V.K. Crosslinked chitosan/polyvinyl alcohol blend beads for removal and recovery of Cd(II) from wastewater. *J. Hazard. Mater.* **2009**, *172*, 1041–1048. [CrossRef] [PubMed]

7. Granados-Correa, F.; Corral-Capulin, N.G.; Olguín, M.T.; Acosta-León, C.E. Comparisonof the Cd (II) adsorption processes between boehmite (γ-AlOOH) and goethite (α-FeOOH). *Chem. Eng. J.* **2011**, *171*, 1027–1034. [CrossRef]
8. World Health Organization (WHO). *Guidelines for Drinking Water Quality: Recommendations*, 3rd ed.; World Health Organization: Geneva, Switzerland, 2008; Volume 1.
9. Kadirvelu, K.; Namasivayam, C. Activated carbon from coconut coirpith as metal adsorbent: Adsorption of Cd (II) from aqueous solution. *Adv. Environ. Res.* **2003**, *7*, 471–478. [CrossRef]
10. Pourrut, B. Implication du Stress Oxydatif Dans la Toxicité du Plomb Sur Une Plante Modèle, Vicia Faba. Ph.D. Thesis, Institut National Polytechnique de Toulouse, Toulouse, France, 2008.
11. Navarro, R.R.; Wada, S.; Tatsumi, K. Heavy metal precipitation by polycation-polyanion complex of PEI and its phosphonomethylated derivative. *J. Hazard. Mater.* **2005**, *123*, 203–209. [CrossRef] [PubMed]
12. Grader, C.; Buhl, J. The intermidiate phase between sodalite and cancrinite: Synthesis of nano-crystals in the presence the Na_2CO_3/TEA and its themal and hydrothermal stability. *Microporous Mesoporous Mater.* **2013**, *171*, 110117. [CrossRef]
13. Nguyen, T.C.; Loganothan, P.; Nguyen, T.V.; Vigneswaram, S.; Kandasamy, J.; Nadu, R. Simultaneous adsorption of Cd, Cr, Cu, Pb, and Zn by an iron-coated Australian zeolite in batch and fixed-bed column studies. *Chem. Eng. J.* **2015**, *270*, 393–404. [CrossRef]
14. Alshameri, A.; Yan, C.; Al-Ani, Y.; Dawood, A.S.; Ibrahim, A.; Zhou, C.; Wang, H.Q. An investigation into the adsorption removal of ammonium by salt activated Chinese (Hulaodu) natural Zeolite: Kinetics, isotherms, and thermodynamics. *J. Taiwan Inst. Chem. Eng.* **2014**, *45*, 554–564. [CrossRef]
15. Zhao, Y.F.; Zhang, B.; Zhang, X.; Wang, J.H.; Liu, J.D.; Chen, R.F. Preparation ofhighly ordered cubic NaA zeolite from halloysite mineral for adsorption of ammonium ions. *J. Hazard. Mater.* **2010**, *178*, 658–664. [CrossRef]
16. Noureddine, H.; Ezzeddine, S. Removal of phosphate ions from aqueous solution using Tunisian clays minerals and synthetic zeolite. *J. Environ. Sci.* **2012**, *24*, 617–623.
17. Wernert, V.; Schaf, O.; Ghobarkar, H.; Denoyel, R. Adsorption properties of zeolites for artificial kidney applications. *J. Microporous Mesoporous Mater.* **2005**, *83*, 101–113. [CrossRef]
18. Hua, R.; Li, Z. Sulfhydryl functionalized hydrogel with magnetism, synthesis, characterization and adsorption behavior study for heavy metal removal. *J. Chem. Eng.* **2014**, *249*, 189–200. [CrossRef]
19. Adam, M.R.; Salleh, N.M.; Othman, M.H.D.; Matsuura, T.; Ali, M.H.; Puteh, M.H.; Jaafar, J. The adsorptive removal of chromium (VI) in aqueous solution by novel natural zeolite based hollow fibre ceramic membrane. *J. Environ. Manag.* **2018**, *224*, 252–262. [CrossRef]
20. Wibowo, E.; Rokhmat, M.; Abdullah, M. Reduction of seawater salinity by natural zeolite (Clinoptilolite): Adsorption isotherms, thermodynamics and kinetics. *Desalination* **2017**, *409*, 146–156. [CrossRef]
21. Yuna, Z. Review of the natural, modified, and synthetic zeolites for heavy metals removal from wastewater. *Environ. Eng. Sci.* **2016**, *33*, 443–454. [CrossRef]
22. Zayed, A.M.; Selim, A.Q.; Mohamed, E.A.; Wahed, M.S.A.; Seliem, M.K.; Sillanpää, M. Adsorption characteristics of Na-A zeolites synthesized from Egyptian kaolinite for manganese in aqueous solutions: Response surface modeling and optimization. *Appl. Clay Sci.* **2017**, *140*, 17–24. [CrossRef]
23. Tauanov, Z.; Tsakiridis, P.E.; Mikhalovsky, S.V.; Inglezakis, V.J. Synthetic coal fly ash-derived zeolites doped with silver nanoparticles for mercury (II) removal from water. *J. Environ. Manag.* **2018**, *224*, 164–171. [CrossRef]
24. Ghrib, Y.; Frini-Srasra, N.; Srasra, E.; Martínez-Triguero, J.; Corma, A. Synthesis of cocrystallized USY/ZSM-5 zeolites from kaolin and its use as fluid catalytic cracking catalysts. *Catal. Sci. Technol.* **2018**, *8*, 716–725. [CrossRef]
25. Pavelić, S.K.; Medica, J.S.; Gumbarević, D.; Filošević, A.; Pržulj, N.; Pavelić, K. Critical Review on Zeolite Clinoptilolite Safety and Medical Applications in vivo. *Front. Pharmacol.* **2019**, *9*, 1350. [CrossRef]
26. Miyake, M.; Akachi, T.; Matsuda, M. Preparation, structure and photocatalytic properties of cancrinite encapsulating lead and sulfide ions. *J. Mater. Chem.* **2005**, *15*, 791. [CrossRef]
27. World Health Organization. Guidelines for Drinking-Water Quality: Incorporating First Addendum. 2017. Available online: http://www.who.int/water_sanitation_health/dwq/gdwq0506.pdf (accessed on 3 April 2018).
28. Denoyel, R.; Giordano, F.; Rouquerol, J. Thermodynamic study of non-ionic-anionic surfactant mixtures: Micellization and adsorption on silica. *Colloids Surf. Physicochem. Eng. Asp.* **1993**, *76*, 141–148. [CrossRef]
29. Denoyel, R.; Rouquerol, F.; Rouquerol, J. Thermodynamics of adsorption from solution: Experimental and formal assessment of the enthalpies of displacement. *J. Colloid Interface Sci.* **1990**, *136*, 375–384. [CrossRef]
30. Ayari, F.; Srasra, E.; Trabelsi-Ayadi, M. Characterization of bentonitic clays and their use as adsorbent. *Desalination* **2005**, *185*, 391–397. [CrossRef]
31. Wang, Z.; Liao, L.; Hursthouse, A.; Song, N.; Ren, B. Sepiolite-based adsorbents for the removal of potentially toxic elements from water: A strategic review for the case of environmental contamination in Hunan, China. *Int. J. Environ. Res. Public Health* **2018**, *15*, 1653. [CrossRef] [PubMed]
32. Esaifan, M.; Warr, L.N.; Grathoff, G.; Meyer, T.; Schafmeister, M.T.; Kruth, A.; Testrich, H. Synthesis of Hydroxy-Sodalite/Cancrinite Zeolites from Calcite-Bearing Kaolin for the Removal of Heavy Metal Ions in Aqueous Media. *J. Miner.* **2019**, *9*, 484. [CrossRef]
33. Rybicka, E.H.; Calmano, W.; Breeger, A. Heavy metals sorption/desorption on competing clay minerals; an experimental study. *Appl. Clay Sci.* **1995**, *9*, 369–381. [CrossRef]

34. Gupta, S.; Bhattacharyya, K. Removal of Cd(II) from aqueous solution by kaolinite, montmorillonite and their poly(oxo zirconium) and tetrabutylammonium derivatives. *J. Hazard. Mater.* **2006**, *128*, 247–257. [CrossRef]
35. Kriaa, A.; Ben Saad, K.; Hamzaoui, A.H. Synthesis and Characterization of Cancrinite Type Zeolite, and Its Ionic Conductivity Study by AC Impedance Analysis. *Russ. J. Phys. Chem.* **2012**, *86*, 2024–2032. [CrossRef]
36. Barnes, M.C.; Addai-Mensah, J.; Gerson, A.R. The mechanism of the sodalite-to-cancrinite phase transformation in synthetic spent bayer liquor. *Microporous Mesoporous Mater.* **1999**, *31*, 287–302. [CrossRef]
37. Kowalak, S.; Jankowska, A.; Zeidler, S. Ultramarine analogs synthesized from cancrinite. *Microporous Mesoporous Mater.* **2006**, *93*, 111–118. [CrossRef]
38. Lin, D.-C.; Xu, X.-W.; Zuo, F.; Long, Y.-C. Crystallization of JBW, CAN, SOD and ABW type zeolite from transformation of meta-kaolin. *Microporous Mesoporous Mater.* **2004**, *70*, 63–70. [CrossRef]
39. Sari, A.; Tuzen, M.; Citak, D.; Soylak, M. Equilibrium, kinetic and thermodynamic studies of adsorption of Pb(II) from aqueous solution onto Turkish kaolinite clay. *J. Hazard. Mater.* **2007**, *149*, 283–291. [CrossRef] [PubMed]
40. Chen, H.; Wang, A. Kinetic and isothermal studies of lead ion adsorption onto palygorskite clay. *J. Colloid Interface Sci.* **2007**, *307*, 309–316. [CrossRef] [PubMed]
41. Borhade, A.V.; Kshirsagar, T.A.; Dholi, A.G.; Agashe, J.A. Removal of Heavy Metals Cd^{2+}, Pb^{2+}, and Ni^{2+} From Aqueous Solutions Using Synthesized Azide Cancrinite, $Na_8[AlSiO_4]_6(N_3)_{2.4}(H_2O)_{4.6}$. *J. Chem. Eng. Data* **2015**, *60*, 586–593. [CrossRef]
42. Elwakeel, K.Z.; El-Bindary, A.A.; Kouta, E.Y. Retention of copper, cadmium and lead from water by Na-Y-Zeolite confined in methyl methacrylate shell. *J. Environ. Chem. Eng.* **2017**, *5*, 3698–3710. [CrossRef]
43. Mihajlović, M.T.; Lazarević, S.S.; Janković-Častvan, I.M.; Kovač, J.; Jokić, B.M.; Janaćković, D.T.; Petrović, R.D. Kinetics, thermodynamics, and structural investigations on the removal of Pb^{2+}, Cd^{2+}, and Zn^{2+} from multicomponent solutions onto natural and Fe(III)-modified zeolites. *Clean Technol. Environ. Policy* **2015**, *17*, 407–419. [CrossRef]
44. Unuabonah, E.I.; Adebowale, K.O.; Olu-Owolabi, B.I. Kinetic and thermodynamic studies of the adsorption of lead (II) ions onto phosphate-modified kaolinite clay. *J. Hazard. Mater.* **2007**, *144*, 386–395. [CrossRef] [PubMed]
45. Hui, K.S.; Chao, C.Y.H.; Kot, S.C. Removal of mixed heavy metal ions in wastewater by zeolite 4A and residual products from recycled coal fly ash. *J. Hazard. Mater.* **2005**, *127*, 89–101. [CrossRef]
46. Ianăşi, C.; Picioruş, M.; Nicola, R.; Ciopec, M.; Negrea, A.; Nižňanský, D.; Len, A.; László Almásy, L.; Putz, A.M. Removal of cadmium from aqueous solutions using inorganic porous nanocomposites. *Korean J. Chem. Eng.* **2019**, *36*, 688–700. [CrossRef]
47. Al-Saida, B.; Sandouqa, A.; Shawabkeh, R.A.; Ibnelwaleed, H. Synthesis of Nanosilica for the Removal of Multicomponent Cd^{2+} and Cu^{2+} from Synthetic Water: An Experimental and Theoretical Study. *J. Mol.* **2022**, *27*, 7536. [CrossRef]
48. Ahmaruzzaman, M. Industrial wastes as low-cost potential adsorbents for the treatment of wastewater laden with heavy metals. *Adv. Colloid Interface Sci.* **2011**, *166*, 36–59. [CrossRef]